Combined MMSE Interference Suppression and Turbo Coding for a Coherent DS-CDMA System

Kai Tang, *Student Member, IEEE*, Laurence B. Milstein, *Fellow, IEEE*, and Paul H. Siegel, *Fellow, IEEE*

***Abstract*—The performance of a turbo-coded code division multiaccess system with a minimum mean-square error (MMSE) receiver for interference suppression is analyzed on a Rayleigh fading channel. In order to accurately estimate the performance of the turbo coding, two improvements are proposed on the conventional union bounds: the information of the minimum distance of a particular turbo interleaver is used to modify the average weight spectra, and the tangential bound is extended to the Rayleigh fading channel. Theoretical results are derived based on the optimum tap weights of the MMSE receiver and maximum-likelihood decoding. Simulation results incorporating iterative decoding, RLS adaptation, and the effects of finite interleaving are also presented. The results show that in the majority of the scenarios that we are concerned with, the MMSE receiver with a rate-1/2 turbo code will outperform a rate-1/4 turbo code. They also show that, for a bit error rate lower than 10^{-3}, the capacity of the system is increased by using turbo codes over convolutional codes, even with small block sizes.**

***Index Terms*—Code division multiple access (CDMA), interference suppression, land mobile radio cellular systems, turbo codes.**

I. Introduction

THE CAPACITY of a DS-code division multiple access (DS-CDMA) system is primarily limited by multiple access interference (MAI) and multipath fading. Various multiuser receivers for DS-CDMA systems have been considered over the past few years. In [1], the performance of a convolutionally coded CDMA system with a minimum-mean-square error (MMSE) receiver for interference suppression has been analyzed. The tradeoff between the time diversity, achieved by convolutional coding and interleaving, and the interference suppression, achieved by the adaptive MMSE receiver, was studied. It was shown that higher rate convolutional codes may provide superior performance in a CDMA system with an MMSE receiver, in contrast to the situation with a conventional matched-filter (MF) receiver.

Recently, turbo coding has been adopted in wireless communication systems to improve the system quality and capacity. Simulation is typically employed to study the performance, since the conventional union bound based on the concept of "uniform interleaver" [2] becomes useless for signal-to-noise ratios (SNR) lower than the thresholds corresponding to the channel cut-off rates, where our interest lies. In order to apply the union bound analysis to the turbo-coded CDMA system, two improvements are proposed in this paper. First, the minimum distance of a specific interleaver is used to modify the average weight spectra, giving a more accurate estimate for the performance offered by the specific interleaver in the error-floor region. Second, the tangential bound is applied to the Rayleigh fading channel to extend the usefulness of the modified bound to the region below the cutoff rate.

Based on these improvements, we study the performance of a turbo-coded DS-CDMA system with an MMSE receiver on Rayleigh fading channels. The performance tradeoffs associated with the allocation of bandwidth to turbo coding and spreading are investigated. In addition, the performance of the turbo-coded system is compared to that of a convolutionally coded system with comparable hardware complexity.

This paper is organized as follows. The structure of the turbo encoders and the two improvements on the conventional union bound are given in Section II. Section III presents the model of the CDMA system and the analysis of the MMSE receiver. Finally, results and conclusions are provided in Sections IV and V, respectively.

II. Turbo Codes

A. Encoder

The turbo encoder considered in this article consists of two or more identical rate-1/2 recursive systematic convolutional (RSC) encoders, each separated by a pseudorandom interleaver of block size N. The parity bit streams are punctured, if necessary, and then transmitted together with the systematic bit stream. At the end of each transmission block, only the first encoder is driven back to the all-zero state through the transmission of tail-bits, whereas the remaining encoders are not terminated. For the first encoder, the trellis termination scheme of [3] is used, wherein the encoder feedback bit is taken as the encoder input and transmitted together with the parity bits. Therefore, the turbo code with M constituent codes is equivalent to a $(N+M\cdot N(1/r_0-1)+\nu/r_0,\ N)$ block code, where r_0 is the rate of the constituent encoders with puncturing and ν is the degree of the feedforward and feedback polynomials. The overall rate of the code is given by

$$R_c=\frac{N}{N+M\cdot N\left(\frac{1}{r_0}-1\right)+\frac{\nu}{r_0}}\approx\frac{1}{1+M\left(\frac{1}{r_0}-1\right)} \tag{1}$$

Manuscript received May 4, 2000; revised November 1, 2000. This work was supported by the National Science Foundation under Grant NCR-9725568, by the CoRe Program of the State of California, by the Center for Wireless Communications, UCSD, and by the TRW Foundation. This paper was presented in part at the Conference on Information Sciences and Systems (CISS'00), Princeton, NJ, USA, March 15–17, 2000.

The authors are with the Department of Electrical and Computer Engineering, University of California, San Diego, La Jolla, CA 92093-0407 USA (e-mail: ktang@ece.ucsd.edu; milstein@ece.ucsd.edu; psiegel@ece.ucsd.edu).

Publisher Item Identifier S 0733-8716(01)02557-4.

where the approximation is valid for practical values of N, ν, and r_0.

In this paper, turbo codes with different code rates are considered. The first encoder uses two rate-1/2 constituent encoders with the generator matrix $(1, (1+D^2)/(1+D+D^2))$, and the two parity sequences are alternately punctured, yielding the overall rate of approximately 1/2. For the rate-1/4 code, two coding schemes, labeled as code "A" and code "B," are considered. Encoder "A" employs three identical component codes with the generator matrix $(1, (1+D^2)/(1+D+D^2))$, and no puncturing is used. Encoder "B" employs two rate-1/3 constituent codes with generator matrix $(1, (1+D^2)/(1+D+D^2), (1+D)/(1+D+D^2))$ [4]. The second parity bit streams of both constituent codes are punctured alternately, resulting in an overall rate of approximately 1/4. Code "A" is the default rate-1/4 coding scheme for our results, unless otherwise stated.

B. Union Bound

In deriving analytical performance bounds, we assume that a maximum-likelihood (ML) decoder is used to decode the turbo codes. Although in practice an iterative decoder will be used, the bounds are useful at high enough SNR, where empirical evidence indicates that the performance of the ML decoder will be approached as the number of decoding iterations increases.

The word error probability and bit error probability of an (L, N) linear block code can be upper bounded by [5]

$$P_e \leq \sum_{d=d_f}^{L} t_d P_2(d) \tag{2}$$

and

$$P_b \leq \sum_{d=d_f}^{L} b_d P_2(d) \tag{3}$$

respectively, where $P_2(d)$ denotes the pairwise error probability for codewords with Hamming distance d. Here, t_d is the number of codewords with Hamming weight d and b_d is the total weight of the information bits for codewords with Hamming distance d, normalized by the number of information bits per block, N.

The sets of all pairs (d, t_d) and (d, b_d) represent the code weight spectra, which are determined by both the constituent encoders and the structure of the specific permutation. Unfortunately, determining the full weight spectra with a particular permutation is computationally prohibitive for realistic values of N. In [2], a probabilistic permutation called a "uniform interleaver" was introduced, which represents an average of all possible interleaving permutations. The uniform interleaver maps a given input sequence of length N and weight w into all distinct $\binom{N}{w}$ permutations of it with equal probability $1/\binom{N}{w}$.

With the help of a uniform interleaver, the average values of t_d and b_d can be determined. The weight enumerating function of the turbo code, conditioned on the input weight, is defined as

$$A(w, Z) \triangleq \sum_{h} A_{w,h} Z^h \tag{4}$$

where $A_{w,h}$ denotes the number of codewords with input weight w and redundancy weight h, yielding the total weight $d = w + h$. The coefficients $\bar{t}_d$ and $\bar{b}_d$ can be obtained by the relations

$$\bar{t}_d = \sum_{w} A_{w,d-w} \tag{5}$$

and

$$\bar{b}_d = \sum_{w} \frac{w}{N} A_{w,d-w} \tag{6}$$

respectively.

The weight enumerating function $A(w, Z)$ can be expressed in terms of the conditional weight enumerating functions $A^{(i)}(w, Z)$, $i = 1, 2, \ldots, M$, of the M constituent codes according to [2]

$$A(w, Z) = \frac{\prod_i A^{(i)}(w, Z)}{\binom{N}{w}^{M-1}}. \tag{7}$$

Finally, the conditional weight enumerating functions $A^{(i)}(w, Z)$ of the constituent block codes can be derived from the transfer function of the constituent convolutional codes. A computationally efficient algorithm for determining $A^{(i)}(w, Z)$, that takes into account the puncturing scheme, is given in [6].

C. Modified Union Bound

The union bound based on the uniform interleaver represents an average over all possible interleavers, and the simulation results show that particular pseudorandom interleavers usually offer performance close to the average until the error-floor region is reached [2]. In the error-floor region, the performance may differ because of the different values of the free distance produced by different interleavers. The difference can be as great as an order of magnitude, requiring some modifications to the average union bound that reflect properties of the specific interleaver.

Let us take the rate-1/2 code as an example. The minimum free distance among the codes produced by all turbo interleavers, d_f, is found to be 3, corresponding to the pattern $(00\cdots0\,011\,100\cdots00)$ in both the original and permuted input sequences. In the worst case, puncturing may result in redundancy weight of zero from both parity bit streams. However, the probability of choosing a pseudorandom interleaver which gives this minimum distance is small. As proven in [7], the contribution to the free distance from codewords with input weight $w \geq 3$ becomes negligibly small for large block size, N because of the so-called "interleaver gain." As N approaches infinity, the free distance is more likely to be the "effective free distance," defined as the minimum weight among codewords corresponding to input words of weight 2. For our rate-1/2 code, the effective free distance is $2 + 2 + 2 = 6$, with equal contributions of two from the systematic bits and the two punctured parity bit streams. Thus, we expect to find a pseudorandom interleaver resulting in $d_{\min} = 6$ for practical values of N without much difficulty.

For a given value of N, the values of the coefficients $\bar{t}_d$ are usually smaller than unity for the first few terms. However, the

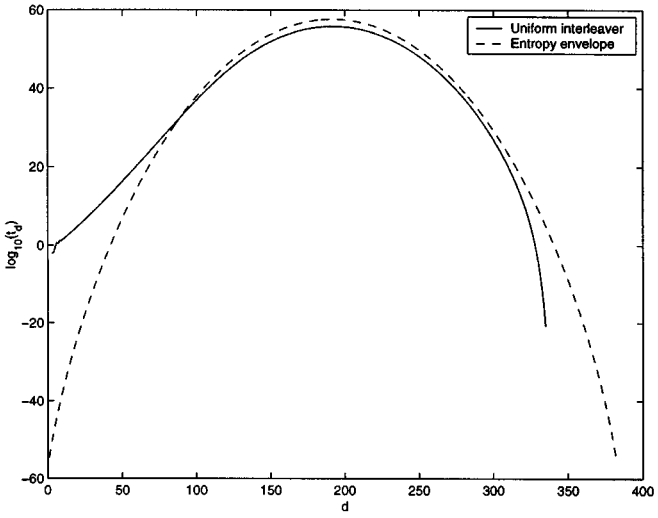

Fig. 1. Weight spectrum based on uniform interleaver for the rate-1/2 turbo code with $N = 190$, compared to the entropy envelope of the random block code.

coefficients t_d corresponding to a particular interleaver always take on integer values. Denote the values t_d for a particular interleaver i as t_d^i, and define $\mathcal{I}_d$ as the set of the interleavers with $t_d^i \neq 0$. We have

$$\bar{t}_d = \frac{1}{N!}\sum_{i=1}^{N!} t_d^i = \frac{1}{N!}\sum_{i\in\mathcal{I}_d} t_d^i \geq \frac{1}{N!}\sum_{i\in\mathcal{I}_d} 1 = \frac{|\mathcal{I}_d|}{N!}. \quad (8)$$

For a particular value of Hamming distance d', if $\sum_{d=d_f}^{d'} \bar{t}_d < 1$, define

$$P_{d'} \triangleq \sum_{d=d_f}^{d'} \bar{t}_d. \quad (9)$$

If we define $\mathcal{I}_{d>d'}$ as the set of interleavers yielding a minimum distance greater than d', the size of $\mathcal{I}_{d>d'}$ is lower bounded by

$$|\mathcal{I}_{d>d'}| \geq N! - \sum_{d=d_f}^{d'} |\mathcal{I}_d| \quad (10)$$

or

$$\frac{|\mathcal{I}_{d>d'}|}{N!} \geq 1 - \frac{1}{N!}\sum_{d=d_f}^{d'} |\mathcal{I}_d| \geq 1 - \sum_{d=d_f}^{d'} \bar{t}_d \geq 1 - P_{d'}. \quad (11)$$

In other words, the probability of randomly choosing an interleaver yielding minimum distance $d_{\min} > d'$ is at least $1 - P_{d'}$. For the rate-1/2 code with $N = 190$, the values of $\bar{t}_d$ are shown in Fig. 1 and the initial terms of the average weight spectrum are shown in Table I. We found $P_5 = \sum_{d=3}^{5} \bar{t}_d \approx 0.39$, which implies that at least 61% of all possible interleavers produce a $d_{\min} \geq 6$, as predicted by the effective free distance.

There are numerous approaches to optimizing the turbo-code interleaver design [3], [8], some of which may lead to $d_{\min}$ even larger than the effective free distance. In our system, we adopted the so-called "S-Random" interleaver [3], which prohibits the mapping of a bit position to another within a distance $\pm S$ of a bit position already chosen in any of the S previous selections. As a rule of thumb, for an interleaver with block size N, $S < \sqrt{N/2}$ is chosen. For the block size $N = 190$, we found such an interleaver with $S = 8$. In our simulation with the particular interleaver, all the error events encountered have Hamming weights at least 8, suggesting $d_{\min} = 8$. We therefore modify the average weight spectrum to reflect the $d_{\min}$ of the specific interleaver, setting

$$t_d = \begin{cases} \bar{t}_d, & d > d_{\min} \\ \sum_{d=d_f}^{d_{\min}} \bar{t}_d, & d = d_{\min} \\ 0, & d < d_{\min}. \end{cases}$$

A similar modification is also applied to each b_d. The union bounds based on the modified weight spectra are shown in Fig. 2. It can be seen that the modification hardly changes the results in the "water-fall" region at lower SNRs but greatly improves the accuracy of the performance estimates in the error-floor region at higher SNRs.

To verify the validity of the proposed modification, we compute a few initial terms of the weight spectra for the rate-1/2 code with the specific S-Random interleaver, using the algorithm in [9]. The true spectra are compared to our modified spectra in Table II, and it is evident why the modified union bounds yield a better estimate for this specific interleaver than the conventional union bounds. The modification to the union bounds is used in the performance analysis that follows.

TABLE I
AVERAGE WEIGHT SPECTRUM FOR THE RATE-1/2 TURBO CODE WITH $N = 190$

d	3	4	5	6	7	8
$\bar{t}_d$	7.9E-3	1.7E-2	3.6E-1	4.6	2.5	13.7
$\bar{b}_d$	1.3E-4	1.9E-4	4.7E-3	4.9E-2	3.6E-2	0.15

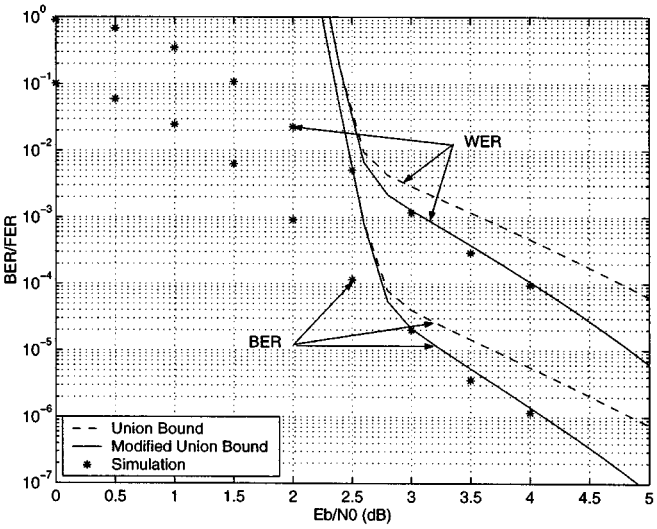

Fig. 2. Comparison between the conventional union bound and the union bound based on the modified weight spectra, for the rate-1/2 turbo code with $N = 190$ on the AWGN channel. Simulation results are also shown.

TABLE II
MODIFIED WEIGHT SPECTRA VERSUS THE ACTUAL WEIGHT SPECTRA FOR THE RATE-1/2 TURBO CODE WITH THE CHOSEN S-RANDOM INTERLEAVER ($d_{\min} = 8$), $N = 190$

d		8	9	10
modified	t_d	21.2	10.2	34.0
average spectra	b_d	0.24	0.16	0.49
actual	t_d	19	3	29
spectra	b_d	0.21	0.03	0.33

D. Tangential Bound

The union bound, by its nature, becomes quite loose at SNRs lower than the threshold corresponding to the channel cutoff rates. There have been several tighter bounds proposed recently [10]–[12], which can be adopted to extend the useful region lower than the cutoff rate on AWGN channels. However, these improved bounds are not readily applicable to wireless communication systems, where fading channels are more typical. In the following, we extend the tangential bound [13], [12] to an ideally interleaved Rayleigh fading channel. The tangential bound is chosen because it offers a balance between computational complexity and the degree of improvement over the union bound. Since only the weight spectrum is needed in the computation, this bound applies to any linear block code, including parallel and serial concatenated turbo codes.

We assume a frequency-flat slow-fading channel. The output of the encoder is mapped to a sequence of BPSK symbols, denoted by an L-dimensional real vector, $\mathbf{x}$. Here L is the number of coded bits per code block and $x_i \in \{\pm 1\}$, $i = 1, \ldots, L$. Assuming a coherent receiver with perfect phase synchronization and no inter-symbol interference (ISI), the received signal is described by

$$y_i = \alpha_i x_i + n_i, \qquad i = 1, \ldots, L \tag{12}$$

where

- $\mathbf{y} = [y_1, y_2, \ldots, y_L]^T$ — L-dimensional received vector;
- $\mathbf{n} = [n_1, n_2, \ldots, n_L]^T$ — random noise vector whose components are independent Gaussian random variables with zero mean and common variance σ^2;
- $\boldsymbol{\alpha} = [\alpha_1, \alpha_2, \ldots, \alpha_L]^T$ — fading amplitude vector consisting of i.i.d. Rayleigh random variables.

We assume the fading amplitudes are normalized so that $E[\alpha_i^2] = 1$, $i = 1, \ldots, L$, and the density of α_i is given by

$$f_\alpha(r) = 2re^{-r^2}, \qquad r \geq 0. \tag{13}$$

The noise variance is determined by $\sigma^2 = 1/2\gamma_c$, where $\gamma_c = E_s/N_0 = R_c E_b/N_0$.

The derivation of the tangential bound over the fading channel closely follows that of the tangential bound on the AWGN channel presented in [12]. The starting point for our derivation is an inequality due to Gallager [14]. Let the event corresponding to an error at the output of the decoder be denoted by $\mathbf{E}$. The probability of decoding error P_e satisfies

$$P_e \leq \Pr[\mathbf{E}, \mathbf{y} \in \mathcal{R}] + \Pr[\mathbf{y} \notin R] \tag{14}$$

where $\mathcal{R}$ is some prespecified region (volume) in the observation space around the transmitted codeword. For the fading channel, the inequality above can be expressed by

$$P_e = E_{\boldsymbol{\alpha}} \Pr[\mathbf{E}|\boldsymbol{\alpha}] \leq E_{\boldsymbol{\alpha}} \Pr[\mathbf{E}, \mathbf{y} \in \mathcal{R}|\boldsymbol{\alpha}] + E_{\boldsymbol{\alpha}} \Pr[\mathbf{y} \notin \mathcal{R}|\boldsymbol{\alpha}] \tag{15}$$

where $E_{\boldsymbol{\alpha}}$ denotes the expectation with respect to the fading vector distribution.

Conditioned on the fading amplitude vector $\boldsymbol{\alpha}$, the mean value of the received vector for each possible codeword has the same energy and is located on an L-dimensional sphere with radius $r = \sqrt{\sum_{i=1}^{L} \alpha_i^2}$, as illustrated in Fig. 3. Let $\mathbf{z}$ be an orthonormal transformation of the noise vector $\mathbf{n}$ so that the components of $\mathbf{z}$ are independent Gaussian random variables with zero mean and the same variance σ^2, but z_1 is directed from the transmitted codeword, $\boldsymbol{\alpha}^T \mathbf{x}_0$, toward the origin. The region $\mathcal{R}$ for the tangential bound is defined as

$$\mathcal{R} = \{\mathbf{y} | z_1 < \rho r\} \tag{16}$$

where ρ is a parameter to be optimized.

The second term on the right-hand side of (15) can be written as [15]

$$\begin{aligned} &E_{\boldsymbol{\alpha}} \Pr[\mathbf{y} \notin \mathcal{R}|\boldsymbol{\alpha}] \\ &\quad = E_{\boldsymbol{\alpha}} \left[Q\left(\frac{\rho r}{\sigma}\right) \right] \\ &\quad = \left(\frac{1-\mu_\rho}{2}\right)^L \sum_{j=0}^{L-1} \binom{L-1+j}{j} \left(\frac{1+\mu_\rho}{2}\right)^j \end{aligned} \tag{17}$$

where

$$\mu_\rho = \sqrt{\frac{\gamma_c \rho^2}{1+\gamma_c \rho^2}}. \tag{18}$$

Alternatively, this term can be represented using another form of the Gaussian Q-function [16]

$$E_{\boldsymbol{\alpha}} \Pr[\mathbf{y} \notin \mathcal{R}|\boldsymbol{\alpha}] = \frac{1}{\pi} \int_0^{\pi/2} \left[1 + \frac{\gamma_c \rho^2}{\sin^2 \phi} \right]^{-L} d\phi. \tag{19}$$

When L is large, this form provides an efficient method to evaluate (17).

Let $\mathbf{E}_d$ denote the event that the received vector is closer to some codeword $\mathbf{x}_j$ at Hamming distance d from the transmitted codeword $\mathbf{x}_0$, than to $\mathbf{x}_0$ itself. The distance between $\boldsymbol{\alpha}^T \mathbf{x}_0$ and $\boldsymbol{\alpha}^T \mathbf{x}_j$ is $l_{0,j} = 2\sqrt{\sum_{i \in \mathcal{X}_{0,j}} \alpha_i^2}$, with $\mathcal{X}_{0,j}$ defined as the set of positions where $\mathbf{x}_j$ differs from $\mathbf{x}_0$: $\mathcal{X}_{0,j} \triangleq \{i\colon x_{0,i} \neq x_{j,i}\}$. The distance l_1 in Fig. 3 is given by

$$l_1 = \sqrt{r^2 - \left(\frac{l_{0,j}}{2}\right)^2} = \sqrt{\sum_{i \notin \mathcal{X}_{0,j}} \alpha_i^2}. \tag{20}$$

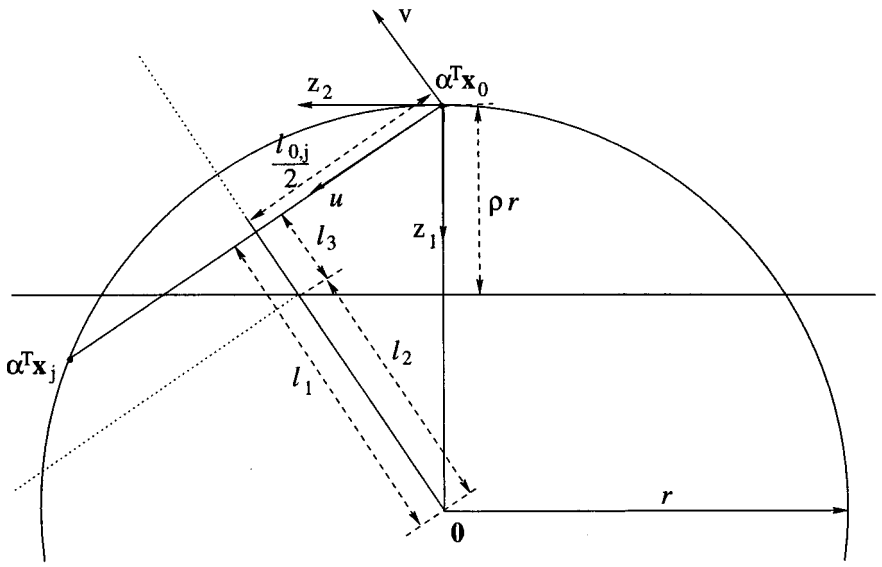

Fig. 3. Illustration of the tangential bound.

For simplicity of notation, we define two random variables

$$\eta_1^{(d)} = \sum_{i \notin \mathcal{X}_{0,\,j}} \alpha_i^2$$

and

$$\eta_2^{(d)} = \sum_{i \in \mathcal{X}_{0,\,j}} \alpha_i^2.$$

They are independent normalized Chi-square random variables with degrees of freedom $2(n-d)$ and $2d$, respectively. Their density functions are given by

$$f_{\eta_1^{(d)}}(x) = \frac{x^{n-d-1}}{(n-d-1)!}\, e^{-x}, \qquad x > 0 \tag{21}$$

$$f_{\eta_2^{(d)}}(x) = \frac{x^{d-1}}{(d-1)!}\, e^{-x}, \qquad x > 0 \tag{22}$$

respectively. Now l_1, $l_{0,\,j}$, and r can be rewritten as

$$l_1 = \sqrt{\eta_1^{(d)}}, \quad l_{0,\,j} = 2\sqrt{\eta_2^{(d)}}, \quad r = \sqrt{\eta_1^{(d)} + \eta_2^{(d)}}. \tag{23}$$

The conditional probability $\Pr[\mathbf{E},\, \mathbf{y} \in \mathcal{R}|\boldsymbol{\alpha}]$ in (15) can be upper bounded by the following union bound:

$$\begin{aligned}\Pr[\mathbf{E},\, \mathbf{y} \in \mathcal{R}|\boldsymbol{\alpha}] &\le \sum_{d=d_{\min}}^{L} t_d \Pr[\mathbf{E}_d,\, z_1 < \rho r|\boldsymbol{\alpha}] \\ &= \sum_{d=d_{\min}}^{L} t_d \Pr\left[u > \frac{l_{0,j}}{2},\, z_1 < \rho r|\eta_1^{(d)},\, \eta_2^{(d)}\right]\end{aligned} \tag{24}$$

where u is the projection of noise along the axis from $\boldsymbol{\alpha}^T\mathbf{x}_0$ to $\boldsymbol{\alpha}^T\mathbf{x}_j$, given by

$$u = \frac{l_{0,j}}{2r}\, z_1 + \frac{l_1}{r}\, z_2. \tag{25}$$

Substitution of (17) and (24) into (15) yields the following tangential bound:

$$\begin{aligned}P_e \le \min_{\rho} \Bigg\{ &\sum_{d=d_f}^{L} t_d E_{\{\eta_1^{(d)},\, \eta_2^{(d)}\}} \\ &\cdot \left[\int_{-\infty}^{\rho r} Q\left(\frac{\sqrt{\eta_2^{(d)}}}{\sigma\sqrt{\eta_1^{(d)}}}(r - z_1)\right) f_z(z_1)\, dz_1\right] \\ &+ \left(\frac{1-\mu_\rho}{2}\right)^L \sum_{j=0}^{L-1} \binom{L-1+j}{j} \left(\frac{1+\mu_\rho}{2}\right)^j \Bigg\}\end{aligned} \tag{26}$$

where $f_z(z_1)$ is the density function of z_1 given by

$$f_z(z_1) = \frac{1}{\sqrt{2\pi}\,\sigma} e^{-z_1^2/2\sigma^2}. \tag{27}$$

By using the axes u and v, (26) can be further simplified. Since

$$\Pr[\mathbf{E},\, \mathbf{y} \in \mathcal{R}|\boldsymbol{\alpha}] \le \sum_{d=d_f}^{L} t_d \Pr\left[u > \frac{l_{0,j}}{2},\, v > -l_3|\eta_1^{(d)},\, \eta_2^{(d)}\right] \tag{28}$$

where the distance l_3 in Fig. 3 is given by

$$l_3 = \frac{1}{\sqrt{\eta_1^{(d)}}}\left[\rho\eta_1^{(d)} - (1-\rho)\eta_2^{(d)}\right] \tag{29}$$

the simplified tangential bound is given by

$$\begin{aligned}P_e \le \min_{\rho} \Bigg\{ &\sum_{d=d_f}^{L} t_d E_{\{\eta_1^{(d)},\, \eta_2^{(d)}\}} \\ &\cdot \left[Q\left(\sqrt{2\gamma_c\eta_2^{(d)}}\right) Q\left(\sqrt{\frac{2\gamma_c}{\eta_1^{(d)}}}\left((1-\rho)\eta_2^{(d)} - \rho\eta_1^{(d)}\right)\right)\right] \\ &+ \left(\frac{1-\mu_\rho}{2}\right)^L \sum_{j=0}^{L-1} \binom{L-1+j}{j} \left(\frac{1+\mu_\rho}{2}\right)^j \Bigg\}.\end{aligned} \tag{30}$$

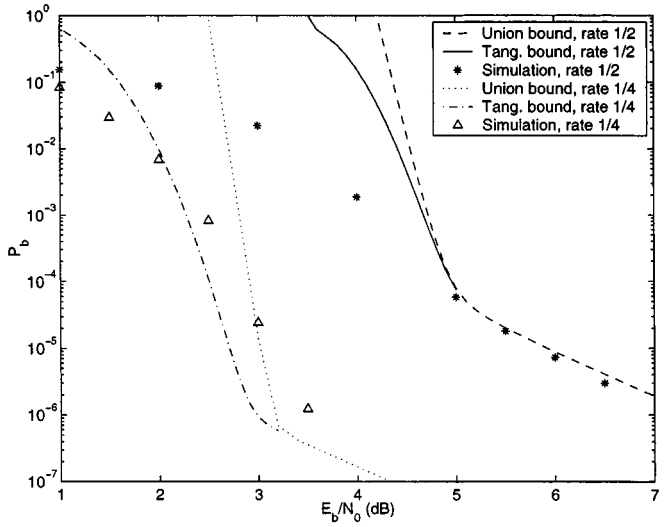

Fig. 4. Comparison between tangential bounds and union bounds on bit error probability of turbo codes over Rayleigh fading, assuming infinite interleaving and perfect CSI. The number of information bits per code block is 190.

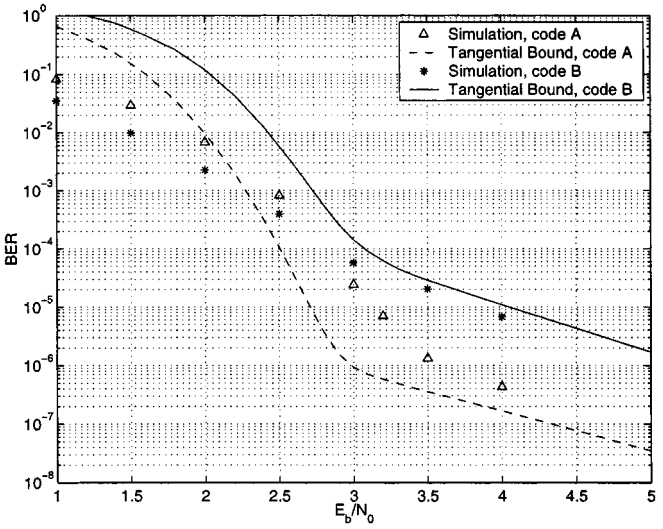

Fig. 5. Comparison between tangential bounds and simulation results on bit error probability of rate-1/4 turbo codes over Rayleigh fading, $N = 190$. Code "A" consists of three component codes, and code "B" consists of two component codes.

When ρ approaches infinity, the tangential bound will become the conventional union bound. This observation shows that the tangential bound is no looser than the union bound. In addition, if ρ approaches minus infinity, only the second term in (30) will remain and this tends to one. So the tangential bound is never larger than one.

Note that in (26) and (30), we choose to optimize over ρ after we remove the conditioning on $\boldsymbol{\alpha}$. Although this choice makes the bound looser, it greatly reduces the computational complexity. The tangential bound can also be extended to other memoryless fading channels in a similar manner.

By replacing t_d with b_d, the tangential bound on the bit error probability is obtained. Fig. 4 compares the tangential bound on the bit error probability with both the union bound and simulation results for a turbo-coded BPSK system over an ideally interleaved Rayleigh fading channel. With the block size $N = 190$, the minimum distances for the rate-1/2 code and the rate-1/4 code "A" with the chosen S-random interleavers are 8 and 22, respectively. The weight spectra are modified accordingly and used in (30) for the tangential bound. As an upper bound on performance of the ML decoder, the tangential bound becomes loose for BER higher than 10^{-4} for the rate-1/2 code. Compared to the conventional union bound, the improvement of the tangential bound is more significant for lower rate codes. Moreover, we observe in the figure that the performance of the iterative decoder may be worse than the tangential bound based on the ML decoder for the rate-1/4 code "A." It is our conjecture that the convergence of the iterative decoder is adversely affected by the fact that there are three constituent codes in code "A." In Fig. 5, the simulation results and tangential bounds are compared for both code "A" and code "B." Since code "B" has only two constituent codes, its error floor is higher than that of code "A." However, code "B" outperforms code "A" for $P_b > 10^{-4}$, and the simulation results for the iterative decoder of code "B" fall below the analytical bound based on the ML decoder.

III. CDMA System

A. System Model

Consider a DS-CDMA system with MMSE interference suppression and turbo coding. The block diagram of the system to be analyzed is shown in Fig. 6. The turbo encoded bits are passed to a channel interleaver. The purpose of the interleaver is to separate adjacent code bits in time, so that, ideally, each code bit will experience independent fading. The output of the interleaver is then mapped to a sequence of QPSK symbols and spread by the signature sequence assigned to the given user. For an asynchronous DS-CDMA system, the transmitted signal for the kth user is given by

$$s_k(t) = \mathrm{Re}\left\{S_k(t)e^{-j\omega_0 t}\right\} \tag{31}$$

where

$$S_k(t) = \sqrt{2P_k}\, a_k(t) b_k(t) \tag{32}$$

P_k is the transmitted power, $b_k(t)$ is the transmitted symbol sequence with period T_s, ω_0 is the carrier frequency, and $a_k(t)$ is the spreading sequence given by

$$a_k(t) = \sum_{i=-\infty}^{\infty} \sum_{n=0}^{N_s-1} a_k^{(n)} h(t - iN_sT_c - nT_c). \tag{33}$$

In (33), $a_k^{(n)} \in \{\pm 1\}$ is the nth chip of the spreading sequence, N_s is the processing gain, $h(t)$ is the impulse response of the chip pulse shaping filter assumed to satisfy the constraint $\int_{-\infty}^{\infty} |H(f)|^2\, df = 1$, and $1/T_c$ is the chip rate. Since it is necessary that the multiple access interference (MAI) statistics be cyclostationary for the MMSE receiver [17], short spreading sequences are used. Therefore $T_s = N_sT_c$.

The channel model assumes slowly varying, frequency nonselective Rayleigh fading along with AWGN. The received signal is given by

$$R(t) = \sum_{k=0}^{K-1} \alpha_k e^{j\psi_k} S_k(t - \tau_k) + N(t) \tag{34}$$

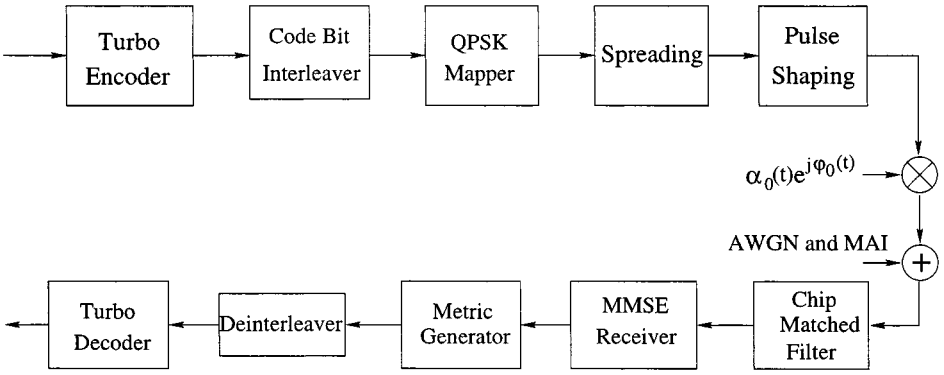

Fig. 6. System model.

where

- K total number of users in the system;
- α_k normalized Rayleigh random variable;
- ψ_k random phase uniformly distributed over $[0, 2\pi)$;
- τ_k delay experienced by the kth user;
- $N(t)$ low-pass equivalent, complex AWGN with $(1/2)E[N(t_1)N^*(t_2)] = N_0\delta(t_1 - t_2)$.[1]

We assume that τ_k is uniformly distributed in the interval $[0, T_s)$ and can be written as $\tau_k = p_kT_c + \delta_k$, where $p_k = 0, 1, \ldots, N_s - 1$ with equal probability, and δ_k is uniform on $[0, T_c)$. Without loss of generality, index $k = 0$ is assigned to the desired user, and we assume perfect bit synchronization (i.e., $\tau_0 = 0$).

After down-conversion, the received signal passes through a chip-matched filter with a normalizing factor of $1/\sqrt{2P_0}\,T_c$, and then a linear adaptive filter with N_s taps [18]. The output of the adaptive filter is fed into a block deinterleaver and an iterative turbo decoder which outputs the estimated data.

B. MMSE Receiver

Assume we can independently track the phase of the desired user and remove it from the received signal prior to entering the MMSE receiver. For the ith code symbol, the output of the coherent demodulator and adaptive filter with tap weights $\mathbf{c}^i$ is given by

$$U_i = (\mathbf{c}^i)^T\mathbf{R}^i_{\mathrm{MF}}e^{-j\psi^i_0} \tag{35}$$

where $\mathbf{R}^i_{\mathrm{MF}} = \mathbf{R}^i_0 + \mathbf{R}^i_N + \mathbf{R}^i_{ma}$, and $\mathbf{R}^i_0$, $\mathbf{R}^i_N$, and $\mathbf{R}^i_{ma}$ are N_s-element column vectors corresponding to the desired user's signal, the AWGN, and the MAI, respectively. It can be shown [1] that

$$\mathbf{R}^i_0 = \alpha^i_0 e^{j\psi^i_0} b^{(i)}_0 \mathbf{a}_0 \tag{36}$$

and

$$\mathbf{R}^i_{ma} = \sum_{k=1}^{K-1} \sqrt{\frac{P_k}{P_0}}\, \alpha^i_k e^{j\psi^i_k}\mathbf{I}^i_k \tag{37}$$

where

$$\mathbf{I}^i_k = \mathbf{d}^{(p_k)}_{k,\,i}\left(1 - \frac{\delta_k}{T_c}\right) + \mathbf{d}^{(p_k+1)}_{k,\,i}\,\frac{\delta_k}{T_c} \tag{38}$$

[1]Following the conventional notations, z^* represents the conjugate of the complex variable z, and $\mathbf{z}^H$ represents the complex conjugate transpose of the complex vector $\mathbf{z}$.

$\mathbf{a}_0 = [a^{(0)}_0, a^{(1)}_0, \ldots, a^{(N_s-1)}_0]^T$, $\mathbf{d}^{(q)}_{k,\,i} = [b^{(i-1)}_k a^{(-q)}_k, b^{(i-1)}_k a^{(-q+1)}_k, \ldots, b^i_k a^{(0)}_k, \ldots, b^i_k a^{(N_s-1-q)}_k]^T$, and $b^{(j)}_k$ is the kth user's symbol transmitted during the time interval $[jT_s, (j+1)T_s)$. The elements in R^i_N are independent complex Gaussian random variables with zero mean and variance $\sigma^2_N = (N_0/E_s)N_s$, where $E_s = P_0T_s$ is the transmitted symbol energy.

The optimum tap weights, which minimize the mean square error $J(i) = E|U_i - b^i_0|^2$ and are found by solving the Wiener–Hopf equation, are given by

$$\mathbf{c}^i_{opt} = R^{-1}_i\mathbf{g}_i \tag{39}$$

where $\mathbf{g}_i \triangleq E[b^{(i)}_0\mathbf{R}^{i*}_{\mathrm{MF}}e^{j\psi^i_0}] = B^i_0\mathbf{a}_0$, and

$$\begin{aligned} R_i &\triangleq E[\mathbf{R}^i_{\mathrm{MF}}\mathbf{R}^{iH}_{\mathrm{MF}}] \\ &= A^i_0\mathbf{a}_0\mathbf{a}^T_0 + \sigma^2_N I_{N_s\times N_s} + \sum_{k=1}^{K-1}\frac{P_k}{P_0}A^i_k E[\mathbf{I}^i_k\mathbf{I}^{iH}_k]. \end{aligned} \tag{40}$$

The two possibilities for A^i_k and B^i_0 depend upon the adaptive receiver's ability to track the time variations of the fading channels. If the fading for the kth user changes relatively fast and cannot be tracked, then $A^i_k = E[(\alpha^i_k)^2]$ and $B^i_k = E[\alpha^i_k]$. If the adaptive algorithm can track the fading on the kth user, then $A^i_k = (\alpha^i_k)^2$ and $B^i_k = \alpha^i_k$.

The following analysis assumes that the receiver has perfect knowledge of the channel state information (CSI) and uses the optimum MMSE filter coefficients, and that infinite interleaving results in independent fades on each symbol. As shown in [1], the output of the adaptive filter can be modeled as a conditionally complex Gaussian random variable as the number of interfering users goes to infinity, based upon the Liapounoff version of the Central Limit theorem [17]. Even for a small number of users, the Gaussian approximation has been shown to yield accurate results [19]. Conditioned on $\{b^{(i)}_0\}$, $\{\alpha^i_0\}$, and $\{\mathbf{c}^i_{opt}\}$, the output of the adaptive filter for the ith symbol is modeled as a complex Gaussian random variable with mean $\mu_i \triangleq E[U_i] = \alpha^i_0 b^{(i)}_0(\mathbf{c}^i_{opt})^T\mathbf{a}_0$ and variance $\sigma^2_{U_i} \triangleq E|U_i - \mu_i|^2 = ((\mathbf{c}^i_{opt})^T\mathbf{a}_0)^2/\mathbf{a}^T_0\tilde{R}^{-1}_i\mathbf{a}_0$, where

$$\tilde{R}_i = I_{N_s\times N_s} + \sum_{k=1}^{K-1}\frac{P_k}{P_0}A^i_k E[\mathbf{I}^i_k\mathbf{I}^{iH}_k]. \tag{41}$$

Conditioning on the optimum tap weights simply refers to conditioning on the delays and on the fades of any interfering users which can be tracked by the adaptive receiver.

C. Bit Error Probability

Following the analysis presented in [1], the conditional probability of pairwise error is given by

$$P_2(d|\{\mathbf{c}_{opt}^i\},\{\alpha_0^i\}) = Q\left(\sqrt{2\gamma_d}\right) \tag{42}$$

where

$$\gamma_d = \sum_{j=1}^{d}\left(\alpha_0^{i_j}\right)^2 \mathbf{a}_0^T \tilde{R}_{i_j}^{-1}\mathbf{a}_0 \tag{43}$$

and $\{i_j: j = 1, 2, \ldots, d\}$ is the set of bit positions over which an erroneous codeword differs from the correct codeword.

We now assume that the adaptive algorithm is not able to track the fading on any of the interfering users in the system, and the delays experienced by each user remain constant throughout a transmission block. These assumptions result in $\tilde{R}_i^{-1}$ being independent of i, and γ_d reduces to

$$\gamma_d = \mathbf{a}_0^T \tilde{R}^{-1}\mathbf{a}_0 \sum_{j=1}^{d}\left(\alpha_0^{i_j}\right)^2 \tag{44}$$

where $\tilde{R} = \tilde{R}_i$ for any i.

Conditioned on $\{\tau_k\}$, the bit error probability $P_e(\{\tau_k\})$ can be obtained by the tangential bound in (30) with equivalent SNR γ_c given by [1]

$$\gamma_c = \tfrac{1}{2}\,\mathbf{a}_0^T \tilde{R}^{-1}\mathbf{a}_0. \tag{45}$$

Averaging $P_e(\{\tau_k\})$ over $\{\tau_k\}$ is done by taking a sample average for various realizations of the delays of all interfering users. Since the calculation of the tangential bound is quite time-consuming, a table of P_e versus the equivalent γ_c is used with linear extrapolation to accomplish the final averaging.

For comparison purposes, we also determined the performance of a matched-filter receiver. If we assume that long spreading sequences are employed and the MAI can be modeled as a Gaussian random variable, the bit error probabilities can be obtained from the tangential bound with γ_c replaced by γ_c^{mf}, where [1]

$$\gamma_c^{mf} = \frac{1}{\dfrac{2N_0}{E_s} + \dfrac{4}{3N_s}\displaystyle\sum_{k=1}^{K-1}\frac{P_k}{P_0}}. \tag{46}$$

IV. Results

We are interested in the coding-spreading tradeoff in a turbo-coded CDMA system. A processing gain of $N_s = 63$ for the uncoded system is assumed. For the MMSE receiver system, the spreading sequences are chosen to be Gold sequences of length 31 for the rate-1/2 codes, and the large set of Kasami sequences of length 15 for the rate-1/4 codes. Therefore, the total bandwidth expansion caused by coding and spreading remains roughly the same.

We assume an SNR of $E_b/N_0 = 15$ dB and perfect power control (i.e., $P_k/P_0 = 1$), unless otherwise specified. The analytical results for the MMSE receiver were obtained by averaging the conditional error probabilities over 1000 realizations of random delays of each user.

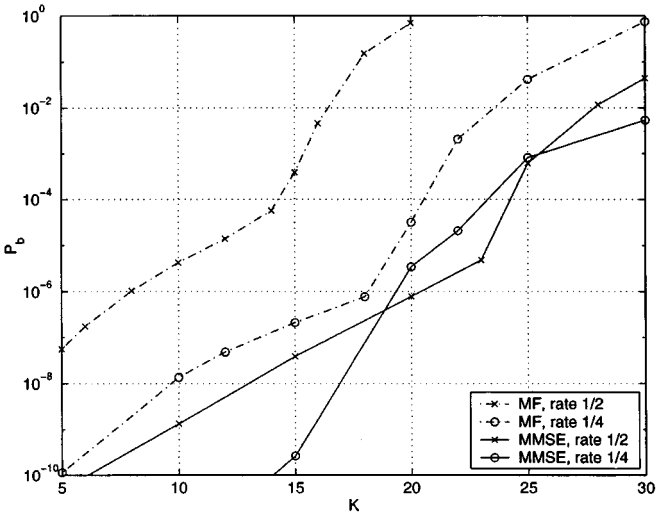

Fig. 7. Comparison between matched-filter receiver and MMSE receiver based on analytical results.

For the simulation of finite interleaving systems, the multipath Rayleigh fading was generated using the Jakes model [20] with a data rate of 9.6 kbps and a maximum Doppler shift of 83 Hz, which corresponds to a carrier frequency of 900 MHz and a vehicle speed of 100 km/h. The number of information bits per block is set to be $N = 190$, corresponding to a tight delay constraint of 20 ms. A block interleaver was used as the channel interleaver, whose dimensions were chosen to be 48×8 and 48×16, for rate-1/2 and rate-1/4 codes, respectively. Dummy bits are appended to each codeword to match the size of the channel interleaver.

In the simulation, the Log-MAP algorithm is used in our iterative decoder [21]. To assure convergence, 15 iterations are used for the rate-1/2 code and the rate-1/4 code "B," and 30 iterations are used for the rate-1/4 code "A." It is claimed in [22] that the processing load of a Log-MAP decoder is no more than four times that of a conventional Viterbi decoder for a convolutional code with the same number of states as the constituent code. So the decoder complexity of the 32-state convolutional codes is approximately the same as that of the rate-1/2 turbo code or the rate-1/4 turbo code "B." For the rate-1/4 code "A," there are 12 states among the three constituent codes, and the decoder complexity is somewhere between that of 32- and 64-state Viterbi decoders. For the comparison, the 32-state convolutional codes of both rates are used.

Fig. 7 compares the analytical results on the bit error probability for the MMSE receiver and the matched-filter receiver with both rate-1/2 and rate-1/4 turbo codes. The results show that the MMSE receiver provides a significant increase in capacity compared to that of the MF system. In addition, although the MF receiver with lower rate codes outperforms that with higher rate codes, the MMSE systems benefit from high-rate codes and larger processing gains when the system is heavily loaded. This is because the number of taps of the MMSE receiver is increased as the processing gain increases, and so the capability to suppress interference is also improved. Note there is a crossing at $K = 26$ of the performance curves for the MMSE receivers with the two code rates, suggesting that when

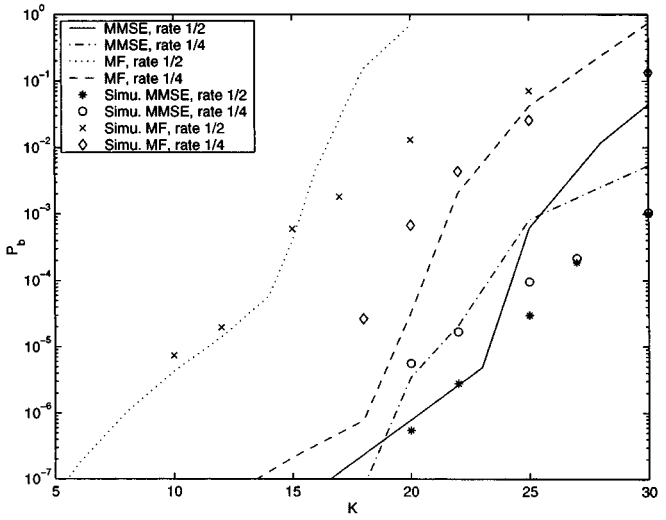

Fig. 8. Comparison between analytical results and simulation for turbo-coded CDMA systems, assuming infinite interleaving and optimum MMSE coefficients.

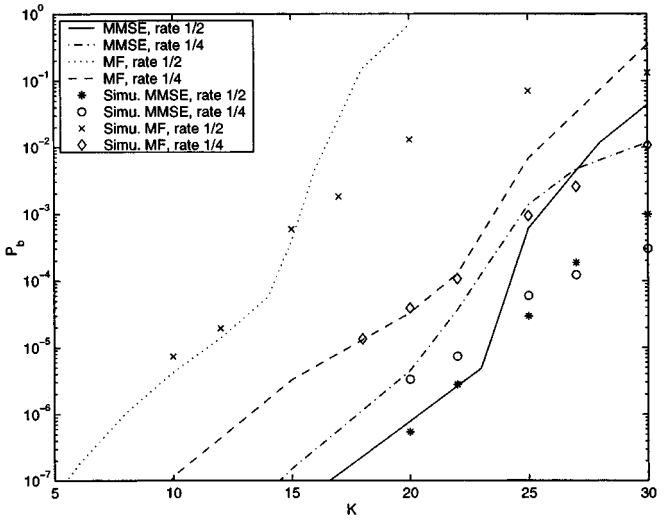

Fig. 9. Comparison between analytical results and simulation for turbo-coded CDMA systems, assuming infinite interleaving and optimum MMSE coefficients. Code "B" is used in the rate-1/4 systems.

the system is operating at a very high capacity (relative to its processing gain), the dimension of the MAI becomes too large for the MMSE receiver to suppress the MAI efficiently and a lower rate code may give better performance.

Fig. 8 compares the analytical results in the previous figure with simulation results. The simulations assume infinite interleaving and optimum tap weights for the MMSE receiver. The simulation results show that our theoretical estimates are good indicators of the performance for low BERs. Since the bound for the turbo codes becomes loose for lower SNRs, the theoretical estimates diverge from the simulation results as the BERs get larger, with the thresholds depending on the coding scheme and the receiver. In particular, we noted that the breakup points for the MMSE receiver are around $P_b \approx 10^{-5}$. It can be seen that the theoretical estimates for the rate-1/4 code are not as accurate as those for the rate-1/2 code, because the tangential bound is not valid for the iterative decoder of code "A," as shown in Fig. 4. Since the Gaussian approximation tends to be optimistic for low BERs [23], the theoretical estimates may be lower than the simulation results for the MF receiver.

In Fig. 9, we substitute code "B" for code "A" in the rate-1/4 systems. The capacity of the system for a target BER of 10^{-4} is improved by the use of code "B." However, both the analysis and simulation show that there is still a range of K over which the MMSE receiver with the rate-1/2 code outperforms that with the rate-1/4 code. We also note that when the system is fully loaded (i.e., K is near 31), the MMSE receiver with the rate-1/4 code "B" gives better performance. As discussed previously, this is because of the large dimensionality of the MAI, and also because of the excellent performance of the rate-1/4 code "B" in the BER range of $P_b > 10^{-4}$.

Fig. 10 analytically compares the performance of the MMSE receivers with code rates of 1/2 and 1/4, with the level of interference varied by changing the power ratio (P_k/P_0) of all the interfering users in the system. Clearly, the rate-1/2 code with the MMSE receiver is more attractive than the rate-1/4 code when the near–far problem is severe.

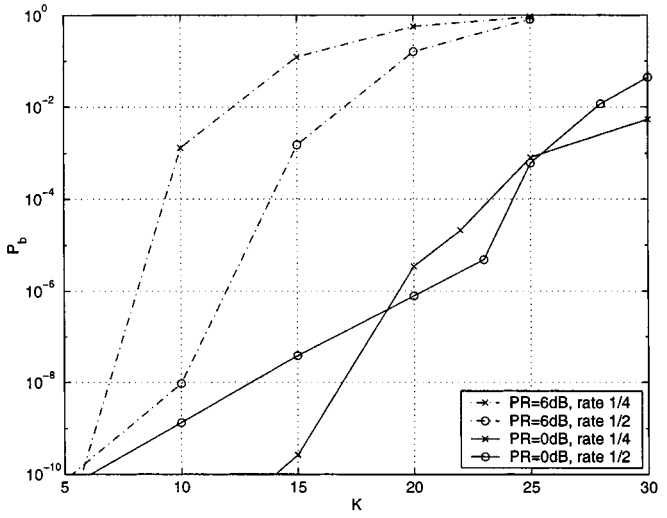

Fig. 10. Performance of MMSE receiver with different code rates and power ratios. $PR = P_k / P_0$ for all interfering users, analytical results.

Fig. 11 compares the performance of turbo-coded CDMA with that of convolutionally coded systems, based on the analytical results. The conventional union bound is applied to the convolutionally coded systems, while the tangential bound for the turbo-coded systems is based on the "uniform interleaver" and the minimum distance of the specific interleaver. Since we are using turbo codes with a relatively small block size, the performances remain approximately the same for the two coding schemes at $P_b = 10^{-3}$, the typical target BER for voice communications. However, for a lower BER (e.g., $P_b = 10^{-5}$), the capacity of the system is significantly increased by using the turbo codes. Moreover, the benefit of turbo codes is more pronounced at larger block sizes, and the turbo-coded systems may outperform the convolutional-coded systems at all BERs for larger block sizes. The result indicates that turbo coding is more suitable for high-speed data communication applications.

Simulation results in Fig. 12 show the performance of the MMSE and MF receivers with finite interleaving and RLS adap-

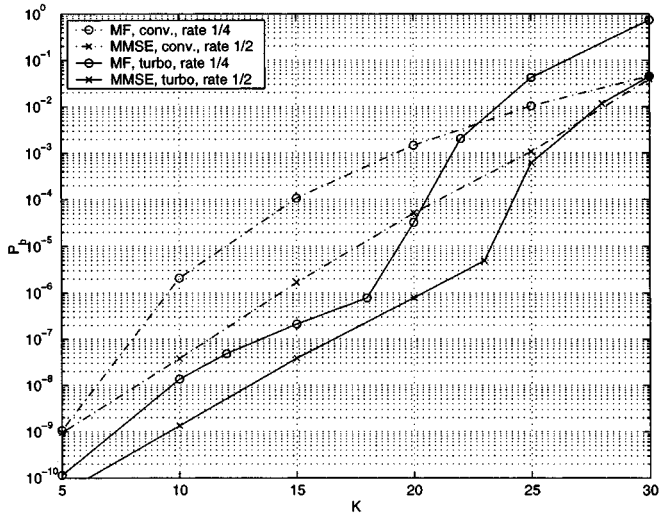

Fig. 11. Comparison between convolutionally coded CDMA and turbo-coded CDMA based on analytical results.

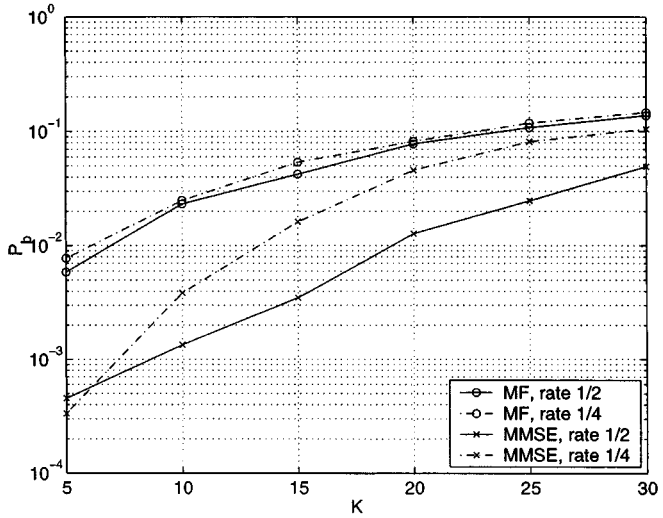

Fig. 12. Simulation results for turbo-coded CDMA systems, assuming finite interleaving (20 ms delay) and RLS adaptation of MMSE coefficients.

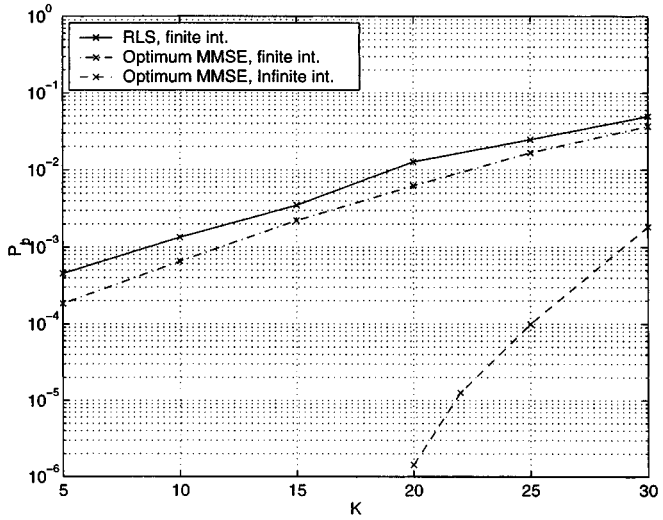

Fig. 13. Simulation results for the MMSE receiver with the rate-1/2 turbo code and various system assumptions.

tation. For our RLS algorithm, $\lambda = 0.995$ is used as the forgetting factor and 300 training symbols are transmitted before decoding user data. The rate-1/2 turbo code with the MMSE receiver is still the best choice. For the MF receiver, the two code rates give approximately the same performance because the advantage arising from the large coding gain of the rate-1/4 code is greatly reduced by the effect of finite interleaving.

Finally, simulation results in Fig. 13 show the degradation of performance for the rate-1/2 turbo-coded system with the MMSE receiver as various system assumptions are removed. The biggest reduction of capacity results from finite interleaving, which shows that the delay constraint is a fundamental limit for reliable communication over fading channels. The figure also shows that when perfect CSI is available, the RLS algorithm is able to closely approximate the performance of the MMSE receiver with optimum tap weights.

V. Conclusion

An extension of the tangential bound is applied to turbo coding on a Rayleigh fading channel, and the actual value of the minimum distance corresponding to a particular turbo interleaver is used to yield more accurate performance in the error-floor region. Theoretical estimates based on these improvements show that the combination of an MMSE receiver and turbo coding can provide a substantial performance improvement compared to conventional matched-filter receiver systems in a multipath fading environment. The MMSE receiver significantly increases the capacity of the system, especially when the near–far problem is severe. For a small block size, turbo codes do not bring much improvement unless a low BER is targeted. Simulation results also show that the system capacity is greatly reduced by the effect of finite interleaving. However, further performance improvement could be expected if looser delay constraints allow the use of turbo codes with larger block size.

References

[1] J. R. Foerster and L. B. Milstein, "Coding for a coherent DS-CDMA system employing an MMSE receiver in a Rayleigh fading channel," *IEEE Trans. Commun.*, vol. 48, pp. 1012–1021, June 2000.

[2] S. Benedetto and G. Montorsi, "Unveiling turbo codes: Some results on parallel concatenated coding schemes," *IEEE Trans. Inform. Theory*, vol. 42, pp. 409–428, Mar. 1996.

[3] D. Divsalar and F. Pollara, "Turbo codes for PCS applications," in *Proc. IEEE Int. Conf. Commun.*, Seattle, WA, June 1995, pp. 54–59.

[4] ——, "On the design of turbo codes," *Telecommunications and Data Acquisition Progress Rep.*, vol. 42, no. 123, pp. 99–121, Nov. 1995.

[5] D. Divsalar, S. Dolinar, F. Pollara, and R. J. McEliece, "Transfer function bounds on the performance of turbo codes," *Telecommunications and Data Acquisition Progress Rep.*, vol. 42, no. 122, pp. 44–55, Aug. 1995.

[6] D. N. Rowitch, "Convolutional and turbo coded multicarrier direct sequence CDMA, and applications of turbo codes to hybrid ARQ communication systems," Ph.D. dissertation, Univ. California San Diego, La Jolla, CA, June 1998.

[7] L. Perez, J. Seghers, and D. J. Costello, Jr., "A distance spectrum interpretation of turbo codes," *IEEE Trans. Inform. Theory*, vol. 42, pp. 1698–1709, Nov. 1996.

[8] J. Yuan, B. Vucetic, and W. Feng, "Combined turbo codes and interleaver design," *IEEE Trans. Commun.*, vol. 47, pp. 484–487, Apr. 1999.

[9] F. Daneshgaran and M. Mondin, "An efficient algorithm for obtaining the distance spectrum of turbo codes," in *Proc. Int. Symp. Turbo Codes Related Topics*. Brest, France, Sept. 1997, pp. 251–254.

[10] T. M. Duman and M. Salehi, "New performance bounds for turbo codes," *IEEE Trans. Commun.*, vol. 46, pp. 717–723, June 1998.

[11] I. Sason and S. Shamai (Shitz), "Improved upper bounds on the ML decoding error probability of parallel and serial concatenated turbo codes via their ensemble distance spectrum," *IEEE Trans. Inform. Theory*, vol. 46, pp. 24–47, Jan. 2000.
[12] H. Herzberg and G. Poltyrev, "The error probability of M-ary PSK block coded modulation schemes," *IEEE Trans. Commun.*, vol. 44, pp. 427–433, Apr. 1996.
[13] E. R. Berlekamp, "The technology of error-correction codes," *Proc. IEEE*, vol. 68, pp. 564–593, May 1980.
[14] R. G. Gallager, *Low Density Parity Check Codes*. Cambridge, MA: MIT Press, 1963.
[15] J. G. Proakis, *Digital Communications*, 3rd ed. New York: McGraw-Hill, 1995.
[16] J. W. Craig, "A new, simple, and exact result for calculating the probability of error for two-dimensional signal constellations," in *Proc. IEEE Military Communications Conf.*, McLean, VA, Oct. 1991.
[17] J. R. Foerster, "The performance of matched-filter and MMSE receivers for DS-CDMA systems in multipath fading channels," Ph.D. dissertation, Univ. California San Diego, La Jolla, Aug. 1998.
[18] S. Miller, "An adaptive direct-sequence code-division multiple-access receiver for multiuser interference rejection," *IEEE Trans. Commun.*, vol. 43, pp. 1746–1755, Feb./March/Apr. 1995.
[19] H. V. Poor and S. Verdu, "Probability of error in MMSE multiuser detection," *IEEE Trans. Inform. Theory*, vol. 43, pp. 858–871, May 1997.
[20] W. C. Jakes, *Microwave Mobile Communications*: IEEE Press, 1974.
[21] S. Benedetto, D. Divsalar, G. Montorsi, and F. Pollara, "Soft-output decoding algorithms in iterative decoding of turbo codes," *Telecommunications and Data Acquisition Progress Rep.*, vol. 42, no. 124, pp. 63–87, Feb. 1996.
[22] A. J. Viterbi, "An intuitive justification and a simplified implementation of the MAP decoder for convolutional codes," *IEEE J. Selected Areas Commun.*, vol. 16, pp. 260–264, Feb. 1998.
[23] R. K. Morrow, Jr. and J. S. Lehnert, "Bit-to-bit error dependence in slotted DS/SSMA packet systems with random signature sequences," *IEEE Trans. Commun.*, vol. 37, pp. 1052–1061, Oct. 1989.

Kai Tang (S'98) received the B.S. and M.S. degrees in electrical engineering from the Southeast University, Nanjing, China, in 1994 and 1997, respectively. Since 1997, he has been a Ph.D. student in electrical engineering at the University of California, San Diego.

His current research interests include spread spectrum communications, multiuser detection, and forward error correction.

Laurence B. Milstein (S'66–M'68–SM'77–F'85) received the B.E.E. degree from the City College of New York, NY, in 1964 and the M.S. and Ph.D. degrees in electrical engineering from the Polytechnic Institute, Brooklyn, NY, in 1966 and 1968, respectively.

From 1968 to 1974, he was with by the Space and Communications Group, Hughes Aircraft Company, and from 1974 to 1976, he was a Member of the Department of Electrical and Systems Engineering, Rensselaer Polytechnic Institute, Troy, NY. Since 1976, he has been with the Department of Electrical and Computer Engineering, University of California at San Diego, La Jolla, where he is a Professor and former Department Chairman, working in the area of digital communication theory with special emphasis on spread-spectrum communication systems. He has also been a consultant to both government and industry in the areas of radar and communications.

Dr. Milstein was an Associate Editor for Communication Theory for the IEEE TRANSACTIONS ON COMMUNICATIONS, an Associate Editor for Book Reviews for the IEEE TRANSACTIONS ON INFORMATION THEORY, an Associate Technical Editor for the IEEE COMMUNICATIONS MAGAZINE, and the Editor-in-Chief of the IEEE JOURNAL ON SELECTED AREAS IN COMMUNICATIONS. He was the Vice President for Technical Affairs in 1990 and 1991 of the IEEE Communications Society and has been a member of the Board of Governors of both the IEEE Communications Society and the IEEE Information Theory Society. He has been a Member of the IEEE Fellows Selection Committee since 1996, and he currently is the Chair of that committee. He is also the Chair of ComSoc's Strategic Planning Committee. He is a recipient of the 1998 MILCOM Long-Term Technical Achievement Award, an Academic Senate 1999 UCSD Distinguished Teaching Award, an IEEE Third Millennium Medal, and the 2000 IEEE Communications Society Edwin Armstrong Achievement Award.

Paul H. Siegel (M'82–SM'90–F'97) received the B.S. degree in mathematics in 1975 and the Ph.D. degree in mathematics in 1979, both from the Massachusetts Institute of Technology. He held a Chaim Weizmann fellowship during a year of postdoctoral study at the Courant Institute, New York University.

He was with the IBM Research Division from 1980 to 1995. He joined the faculty of the School of Engineering at the University of California San Diego, in July 1995, where he is currently Professor of Electrical and Computer Engineering. He is affiliated with the Center for Wireless Communications and became Director of the Center for Magnetic Recording Research in September 2000. His primary research interest is mathematical foundations of signal processing and coding, especially as applicable to digital data storage and communications. He holds several patents in the area of coding and detection for digital recording systems.

Dr. Siegel was a corecipient of the 1992 IEEE Information Theory Society Paper Award and the 1993 IEEE Communications Society Leonard G. Abraham Prize Paper Award. He was a member of the Board of Governors of the IEEE Information Theory Society from 1991 to 1996. He served as co-Guest Editor of the May 1991 Special Issue on "Coding for Storage Devices" of the IEEE TRANSACTIONS ON INFORMATION THEORY, and was Associate Editor for Coding Techniques from 1992 to 1995. He is a member of Phi Beta Kappa.